THE JOURNAL OF PHYSICAL CHEMISTRY C

Article

pubs.acs.org/JPCC

Defect Activated Photoluminescence in WSe_2 Monolayer

Zhangting Wu,[†,∥] Weiwei Zhao,[‡] Jie Jiang,[†] Ting Zheng,[†] Yumeng You,[§] Junpeng Lu,*[,†] and Zhenhua Ni*[,†,∥]

[†]School of Physics, [‡]Jiangsu Key Laboratory for Design and Fabrication of Micro-Nano Biomedical Instruments, School of Mechanical Engineering, and [§]Ordered Matter Science Research Center, Southeast University, Nanjing 211189, People's Republic of China

[∥]State Key Laboratory for Modification of Chemical Fibers and Polymer Materials, Donghua University, 201620, Shanghai, People's Republic of China

ABSTRACT: Defects in transition metal dichalcogenides (TMDs) play an important role in tailoring electrical and optical properties. Here we employ Ar^+ plasma to controllably generate active defects in WSe_2 monolayers to tune their optical properties. Two defect-activated PL emission peaks are emerging in the low temperature PL spectra of WSe_2 monolayer treated with Ar^+ plasma. These emissions are attributed to the recombination of excitons bound to different types of structural defects. The shallow level emission originates from the recombination of excitons at chalcogen vacancies, while the deep level emission might arise from other types of defects, such as transition metal vacancies, cluster of vacancies, rotational defects, or antisite defects. Our results demonstrate that Ar^+ plasma treatment is an effective approach to induce desirable defects in TMDs monolayers and PL spectroscopy is an efficient method to investigate these defects.

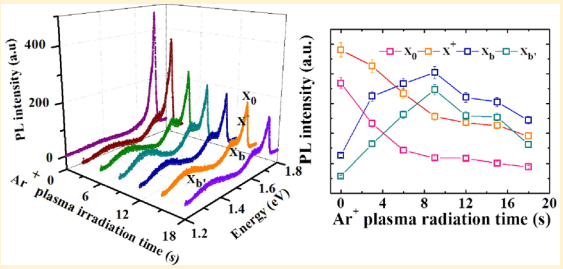

INTRODUCTION

TMDs have been extensively studied due to their interesting optical and electronic properties.[1−3] Especially, their monolayers present strong photoluminescence (PL) and large exciton binding energy.[4−6] This facilitates TMDs monolayers robust applications in photonics and optoelectronics.[7] Despite many devices based on the TMDs, monolayers have been demonstrated to present high performance; the structural defects such as vacancies, adatoms, and substitutional impurities are inevitable in the materials.[8−11] These defects could act as efficient trapping centers for electrons, holes, and excitons and have a strong influence on the electronic and optical properties.[8−16] For example, sulfur vacancies that exist in intrinsic MoS_2 introduce localized donor states inside the bandgap and result in hopping transport at room temperature.[8] In addition, sulfur vacancies could induce the n-doping effect in MoS_2 monolayer and facilitate the formation of negatively charged excitons and reduce the intensity of PL emission.[9] On the other hand, the defects could be inversely a merit instead of the disadvantages. Strong PL enhancement of MoS_2 monolayer has been realized by defect engineering.[9,12] Oxygen adatoms on MoS_2 monolayer could induce the p-doping effect and suppress the nonradiative recombination of excitons at the defect sites.[9] Isoelectronic substitutional oxygen defects improves the conductivity of WSe_2 monolayer by ∼400 times and its photoconductivity by ∼150 times.[10] Therefore, different types of defects in TMDs play different roles, and it is worth to clarify the functionalities of these defects and further to develop an effective approach to control the defects.

Spectroscopic methods, especially PL spectroscopy, are time efficient and sensitive methods to study defects in TMDs.[11,17−19] At low temperature, a strong defect activated PL peak has been identified in naturally MoS_2 monolayer, which is attributed to the emission of exciton bounded to defects or adsorbs.[20] Quantification of defects by PL spectroscopy and their correlation with the electrical performance have been investigated in WSe_2 monolayer.[20] However, the influence of different types of defects to the optical properties of TMDs has yet to be well investigated. Different types of defects can form different localized states in 2D materials, which might render bound exciton emissions with different energies.

In this work, we develop a straightforward and effective method to engineer the defects in WSe_2 monolayer by means of Ar^+ plasma treatment. The effects of the defects on the properties of WSe_2 monolayer are investigated by PL and Raman spectroscopies. We find that the optical property of WSe_2 monolayer can be easily controlled via changing the treatment parameters of Ar^+ plasma. Temperature and power dependent PL spectra indicate that treatments with Ar^+ plasma could introduce different types of defects into the WSe_2 monolayer, and these defects could activate different PL emissions.

Received: April 17, 2017
Revised: May 17, 2017
Published: May 18, 2017

DOI: 10.1021/acs.jpcc.7b03585
J. Phys. Chem. C 2017, 121, 12294−12299

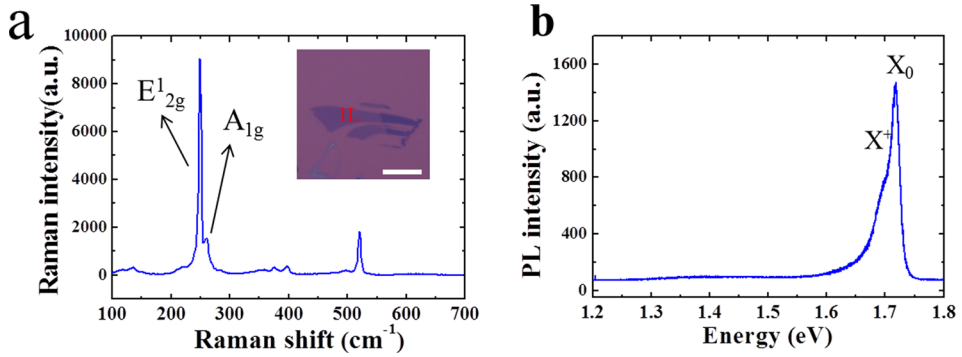

Figure 1. (a) Raman spectrum of WSe_2 monolayer. Inset shows the optical image of sample. Scale bar is 20 μm. (b) PL spectrum of pristine WSe_2 monolayer measured at low temperature of 83 K.

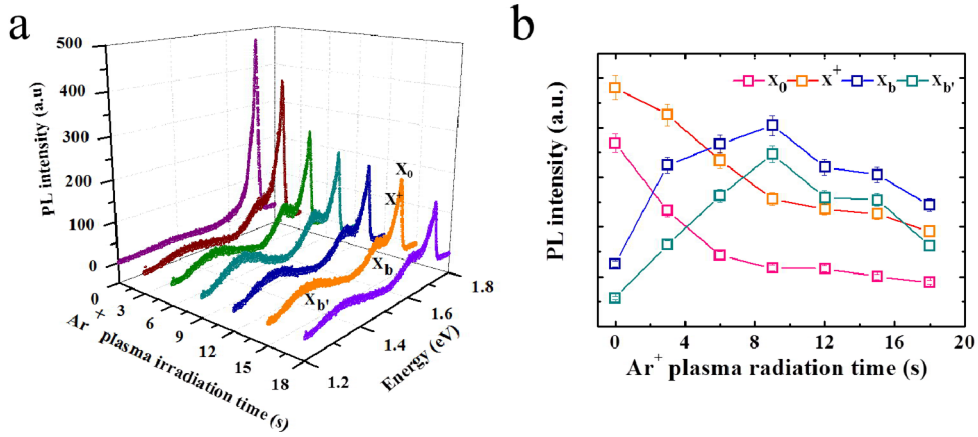

Figure 2. (a) PL spectra of WSe_2 monolayer treated with Ar^+ plasma with different irradiation time. The measurements are carried out at 83 K with laser power of 0.45 μW. (b) The integrated PL intensity of X_0, X^+, X_b, and $X_{b'}$ peaks as a function of irradiation time.

EXPERIMENTAL METHODS

The samples were mechanically exfoliated onto the Si/SiO_2 substrate from WSe_2 crystals (SPI Supplies). The thickness of monolayer WSe_2 was confirmed by optical contrast and Raman spectroscopy.[21] Ar^+ plasma (commercial 13.56 MHz RF source) with power of 5 W was used to irradiate the WSe_2 sheets with different irradiation times at room temperature. The experiments were carried out at a chamber with the pressure of 5 Pa. The Raman and PL spectra were recorded using a LabRAM HR800 Raman system. The wavelength of the excitation laser is 514.5 nm, and the spot size is ~1 μm. Low temperature measurements were performed in an INSTEC HCP621V stage with mk1000 high precision temperature controller and LN2-SYS liquid nitrogen cooling system.

RESULTS

The WSe_2 monolayer was mechanically exfoliated from a WSe_2 crystal. The optical microscopy image of a prepared product is shown in the inset of Figure 1a. Two strong peaks at 248 and 261 cm^{-1} are observed in the Raman spectrum. They can be assigned to E^1_{2g} and A_{1g} modes of WSe_2, respectively.[22] The peak at around 308 cm^{-1} disappears in WSe_2 monolayer while it becomes Raman active in bilayer and thicker samples.[22] The PL spectrum of pristine WSe_2 monolayer measured at 83 K is shown in Figure 1b. Two peaks are observed at ~1.71 and ~1.73 eV. These two peaks have been intensively investigated and arise from the recombination of trions (X^+) and neutral excitons (X_0), respectively.[23]

Following, the WSe_2 monolayer is subjected to the treatment with Ar^+ plasma. The PL spectra of WSe_2 monolayers modified by Ar^+ plasma with increasing irradiation time are recorded and shown in Figure 2a. The measurements are carried out at 83 K with laser power of 0.45 μW. The modified sample presents two additional PL peaks located at ~ l.60 eV (denoted as X_b) and ~1.35 eV (denoted as $X_{b'}$). The presence of the X_b peak indicates the existence of shallow level in the bandgap of WSe_2 monolayer. The energy position of ~1.60 eV is consistent with the electron beam irradiation induced defect level in WSe_2 monolayer.[20] With increasing irradiation time of Ar^+ plasma, the $X_{b'}$ peak emerges. The peak position of ~1.35 eV indicates that a deep defect level is introduced into WSe_2 monolayer. Evidently, a longer exposure time of Ar^+ plasma would generate higher density of defects in WSe_2 monolayer. As summarized in Figure 2b, the PL intensity of X_0 and X^+ decreases with the increasing irradiation time of plasma, indicating that the introduced structural defects could suppress the formation or recombination of neutral excitons and trions, while the intensity of X_b and $X_{b'}$ rises with increasing exposure time. This indicates that more excitons are bounded to the defects and recombine at the defect sites. At even higher exposure time conditions, the intensity of X_b and $X_{b'}$ decreases. This might be due to the increase of nonirradiative recombination of excitons at the presence of very high density of defects.

To obtain a deep insight into the origination of X_b and $X_{b'}$ peaks, laser power and temperature dependent PL spectra are collected from the modified WSe_2 monolayer and shown in Figures 3 and 4, respectively. Since the intensity of X_0 presents

DOI: 10.1021/acs.jpcc.7b03585
J. Phys. Chem. C 2017, 121, 12294−12299

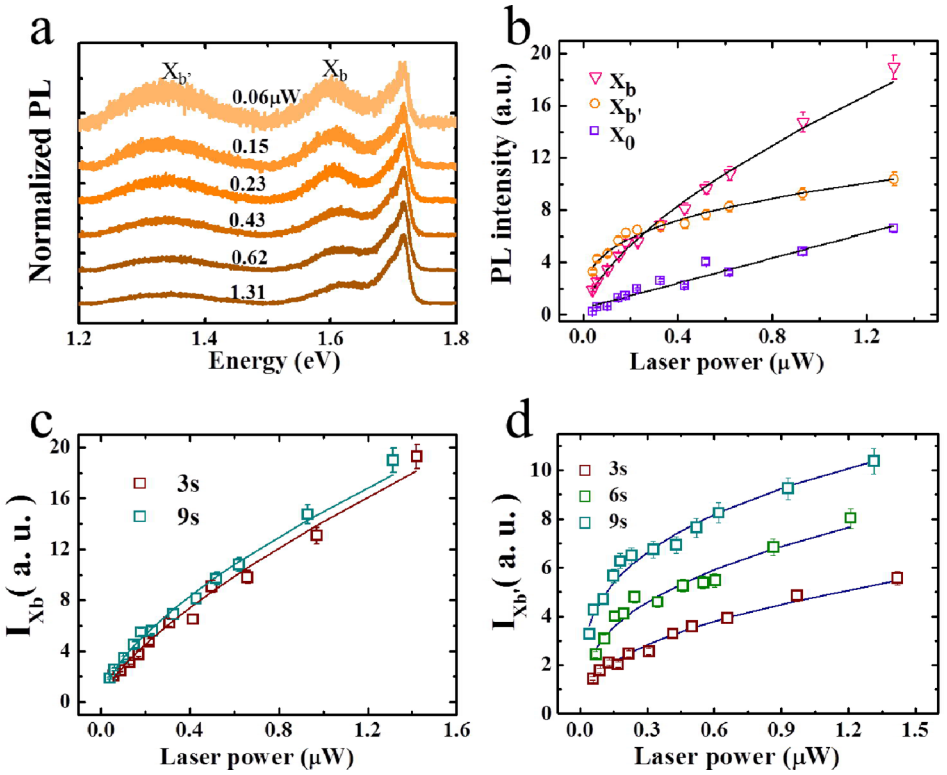

Figure 3. (a) PL spectra (normalized by the intensity of X_0) collected under the excitation with different laser powers. (b) The integrated PL intensity of X_0, X_b, and $X_{b'}$ as a function of laser power. Laser power dependence of integrated intensities of X_b(c) and $X_{b'}$ (d) collected from the sample treated with different irradiation times. The solid curve is the fitting result according to the power law $I \propto P^k$.

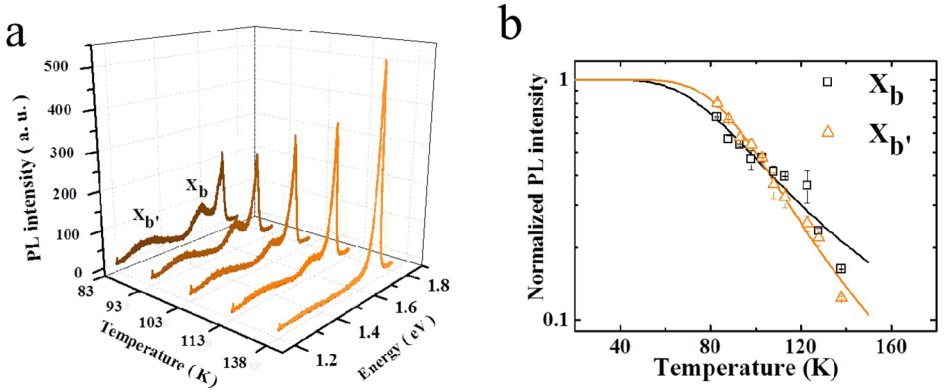

Figure 4. (a) PL spectra of WSe_2 monolayer measured at different temperatures. (b) Intensity of the relative X_b and $X_{b'}$ emission as a function of temperature. The solid curve is the fitting result based on the thermal dissociation model.

linear dependence on incident laser power at lower excitation (<1.5 μW),[24] the PL spectra are normalized by X_0 intensity to emphasize the change of X_b and $X_{b'}$. The peak area (I) of X_b, $X_{b'}$, and X_0 is extracted and plotted as a function of laser power (P) (Figure 3b). Evidently, the variation of both X_b and $X_{b'}$ can be well fitted by power law $I \propto P^k$,[25] where k for X_b is ~0.64 and k' for $X_{b'}$ is ~0.30. This nonlinear dependence shows the tendency of saturation at higher laser power conditions. It can be explained by the full population of defect states with excitons at high excitation power.[20] In particular, the intensity of $X_{b'}$ presents the characteristic saturation behavior earlier than X_b. This indicates that the defect states of deep level are easier to be populated. Namely, the excitons prefer to fill into the defect states at low energy level. Figures 3c and 3d show PL intensity of X_b and $X_{b'}$ as a function of laser power collected from the WSe_2 monolayers modified by Ar^+ plasma with different irradiation times. The extracted experimental data could be fitted well by the same power-law function. The best fitting parameters, k and k', do not exhibit significant changes with increasing plasma irradiation time. This indicates that the amount of Ar^+ plasma irradiation does not alter the nature of induced defects. The saturated PL intensity of X_b and $X_{b'}$ rises with increasing Ar^+ plasma irradiation time, in good accordance with the increase of defect densities.

The temperature dependent PL spectra are collected and shown in Figure 4a.With increasing temperature, the intensity of $X_{b'}$ and X_b decreases while the intensity of X_0 increases. The quenching of PL intensity of X_0 with reducing temperature arises from the presence of dark excitons.[26] The decrease of PL intensity of $X_{b'}$ and X_b peaks with increasing temperature

DOI: 10.1021/acs.jpcc.7b03585
J. Phys. Chem. C 2017, 121, 12294−12299

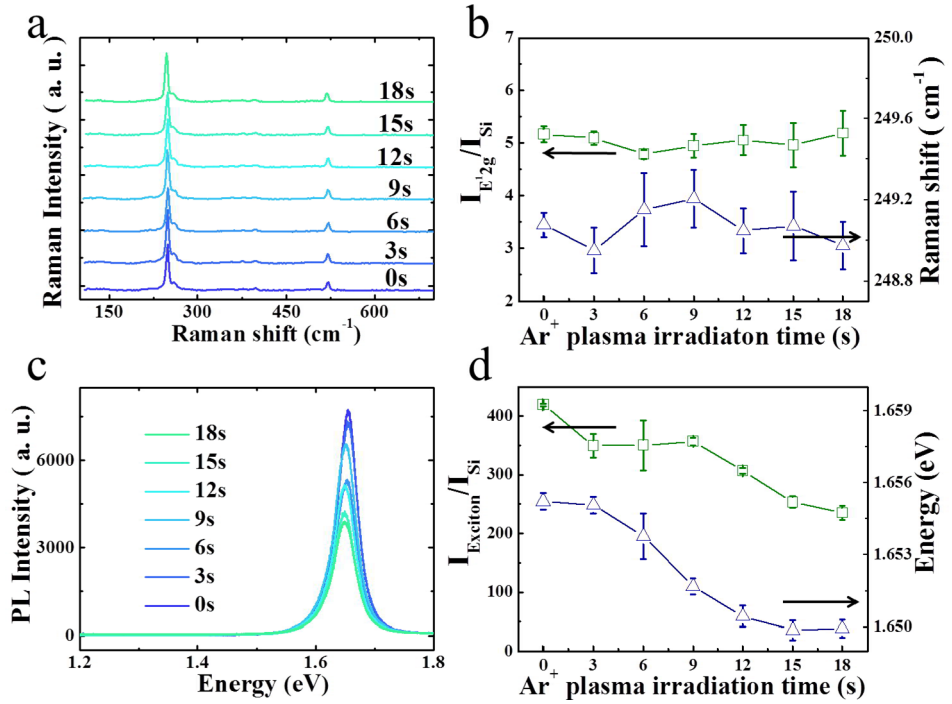

Figure 5. (a) Raman and (c) PL spectra (measured at room temperature) of monolayer WSe_2 treated with Ar^+ plasma with different irradiation time. (b) Raman intensity (normalized by the intensity of Si peak) and position of E^1_{2g} peak as a function of irradiation time. (d) PL intensity (normalized by the intensity of Si peak) and energy of exciton as a function of irradiation time.

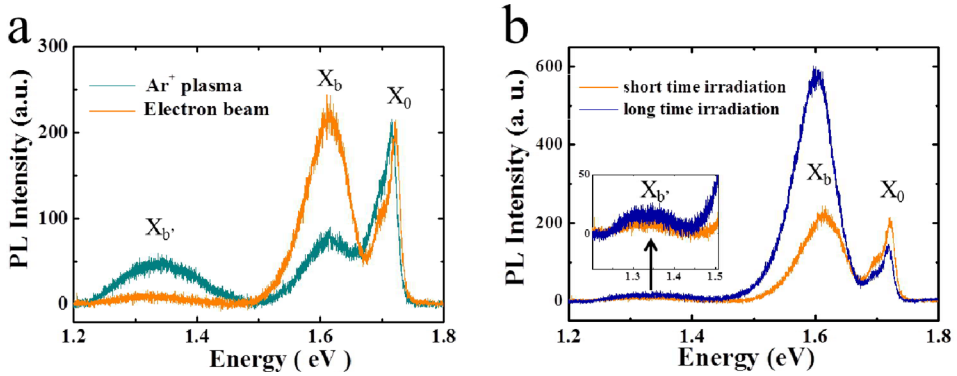

Figure 6. (a) PL spectra of defective WSe_2 monolayers produced by Ar^+ plasms and electron beam irradiation with electron density of 7.28×10^6 μm^{-2}. (b) PL spectra of WSe_2 sample after short (electron density of 7.28×10^6 μm^{-2}) and long (electron density of 49.53×10^6 μm^{-2}) time irradiation of electron beam. The $X_{b'}$ peak appears gradually after long time electron beam irradiation. The inset is a zoom-in of the $X_{b'}$ emission region.

indicates the weak bound energy between excitons and defects. It can be easily perturbed by thermal stimulation.[20] At low temperature, a certain amount of exciton could be captured by defects. As temperature increased, the trapped excitons could be released again from the defect states. The temperature dependence of $X_{b'}$ and X_b can be described by a thermally dissociation process (Figure 4b), $I(T) = \frac{I(0)}{1 + (\tau / \tau_0)e^{-E_A/KT}}$, where $I(0)$ is the PL intensity at $T = 0$ K, τ is the excitonic lifetime, τ_0 is effective scattering time, E_A is activation energy, and K is the Boltzmann constant.[20] By fitting the data in Figure 4b with the equation, the activation energy can be extracted to be ~37.1 meV for X_b and ~54.7 meV for $X_{b'}$. The thermal activation energy is the required energy of thermal perturbation that can prevent the free excitons from trapping of defect states.[20] $X_{b'}$ has a larger activation energy than X_b, suggesting that the excitons require higher energy to be dissociated from the deep level traps.

Figure 5 shows Raman and PL spectra of WSe_2 monolayers modified by Ar^+ plasma with different irradiation times at room temperature. The intensities of PL and Raman peaks are normalized by the silicon peak. Both the intensity and frequency of the Raman peak do not show significant change with plasma irradiation time. This indicates that the lattice of monolayer WSe_2 remains intact after Ar^+ plasma irradiation. However, the intensity of PL peak decreases, and the position red-shifts with increasing Ar^+ plasma irradiation time. The decrease of PL intensity might originate from the introduction of doping and the reduced exciton lifetime.[20,27] Defects induced by plasma treatment can lead to doping of TMDs,[27] while they could also bring in more relaxation channels in TMDs and thus reduce the lifetime of excitons.[20] As known, the presence of

DOI: 10.1021/acs.jpcc.7b03585
J. Phys. Chem. C 2017, 121, 12294−12299

defects in TMDs can also change the band structure and the bandgap, which may be a factor that causes red-shift of the PL peak.[8]

The difference in the peak position of X_b and $X_{b'}$ indicates the recombination of excitons at different defect levels. Theoretical calculations show that the energy and strength of midgap states localized around defects depend on the specific missing atoms, their concentration, and the specific arrangement of the point defects.[28] Many defective TMDs samples have been reported to present PL peaks similar to X_b.[12] They were attributed to the recombination of excitons bounded to mid-bandgap states with energies of ∼0.1−0.3 eV above the valence band maximum or below the conduction band minimum. A significant defect-induced PL emission has been observed in the low temperature PL spectrum of WSe_2 monolayer processed with electron beam lithography (EBL).[20] This emission has the similar peak position to the X_b peak. It is suggested that this peak originates from the excitons bounded to structural defects (vacancies) rather than other defects of charged impurities or adsorbates.[20] For comparison, we collect PL spectra on WSe_2 monolayers treated with electron beam and Ar^+ plasma, respectively (Figure 6a). The measurements are carried out at 83 K with laser power of 0.45 μW. Evidently, the treatment with Ar^+ plasma could facilitate X_b and $X_{b'}$ peaks while electron beam treatment only induced the strong X_b peak. The results indicate that Ar^+ plasma is a more effective approach to generate and control the structural defects in TMDs monolayers as compared to electron beam.

DISCUSSION

According to previous studies, the irradiation of low-energy electron beam could mainly introduce vacancy defects in TMDs.[29] The electron-irradiation-induced chalcogen vacancies have been observed via high-resolution transmission electron microscopy (HRTEM) in MoS_2 monolayer.[29] Line defects consisted of a row of single vacancies could be even formed under higher power of electron beam irradiation.[30] In addition to the chalcogen vacancy, more complex defects could be introduced into the TMDs monolayers via higher energy or longer time electron irradiation. These defects can introduce deep level localized states and therefore the emergence of a weak peak at ∼1.35 eV (Figure 6b). Compared to the results of Ar^+ plasma irradiation, the peak position is consistent with $X_{b''}$. However, the peak intensity is much lower than $X_{b'}$ induced by Ar^+ plasma. This further demonstrates that Ar^+ plasma treatment is a more effective technique to generate deep level defects in TMDs monolayers. The deep level defects corresponding to $X_{b''}$ peak might be transition metal vacancies, cluster of vacancies, rational defects, or antisite defects in WSe_2 monolayer. Metal atoms vacancies and cluster of vacancy defects have been demonstrated to present the capability to facilitate deep level localized states.[28] Studies have found that rotational defect formed by a 60° rotation of three bonds centered on a metal atom in WSe_2 at elevated temperature or under high-energy electron beam irradiation, which facilitate additional states in the midgap.[31] In addition, according to the theoretical prediction, antisite defects, such as Mo atom substitution of S atom(s) included Mo_S and Mo_{S2} in MoS_2 sample, facilitate defect states with nearly flat band dispersion inside the bandgap.[32]

CONCLUSIONS

In summary, we have demonstrated that Ar^+ plasma irradiation could generate different kinds of defects into the WSe_2 monolayer, and these defects could active different PL emissions. The species of defects can be easily engineered via changing the treatment parameters of Ar^+ plasma. In doing so, the optical property of WSe_2 monolayer would be consequently modified. The varieties of the defects and the effects of the defects on the optical properties are clarified by the PL spectroscopic measurements at low temperature.

AUTHOR INFORMATION

Corresponding Authors

*E-mail: zhni@seu.edu.cn (Z.N.).
*E-mail: phyljp@seu.edu.cn (J.L.).

ORCID

Zhenhua Ni: 0000-0002-6316-2256

Notes

The authors declare no competing financial interest.

ACKNOWLEDGMENTS

This work is supported by National Natural Science Foundation of China (Nos. 61422503, 21541013, and 61376104), Natural Science Foundation of Jiangsu Province (No. BK20150596), the open research funds of Key Laboratory of MEMS of Ministry of Education (SEU, China), and the Fundamental Research Funds for the Central Universities.

REFERENCES

(1) Radisavljevic, B.; Radenovic, A.; Brivio, J.; Giacometti, V.; Kis, A. Single-layer MoS_2 transistors. *Nat. Nanotechnol.* **2011**, *6*, 147−150.

(2) Wang, Q. H.; Kalantarzadeh, K.; Kis, A.; Coleman, J. N.; Strano, M. S. Electronics and optoelectronics of two-dimensional transition metal dichalcogenides. *Nat. Nanotechnol.* **2012**, *7*, 699−712.

(3) Lopezsanchez, O.; Lembke, D.; Kayci, M.; Radenovic, A.; Kis, A. Ultrasensitive photodetectors based on monolayer MoS_2. *Nat. Nanotechnol.* **2013**, *8*, 497−501.

(4) Zhao, W.; Ghorannevis, Z.; Chu, L.; Toh, M.; Kloc, C.; Tan, P. H.; Eda, G. Evolution of electronic structure in atomically thin sheets of WS_2 and WSe_2. *ACS Nano* **2013**, *7*, 791−797.

(5) Hanbicki, A. T.; Currie, M.; Kioseoglou, G.; Friedman, A. L.; Jonker, B. T. Measurement of high exciton binding energy in the monolayer transition-metal dichalcogenides WS_2 and WSe_2. *Solid State Commun.* **2015**, *203*, 16−20.

(6) Huang, J.; Hoang, T. B.; Mikkelsen, M. H. Probing the origin of excitonic states in monolayer WSe_2. *Sci. Rep.* **2016**, *6*, 22414.

(7) Mak, K. F.; Shan, J. Photonics and optoelectronics of 2D semiconductor transition metal dichalcogenides. *Nat. Photonics* **2016**, *10*, 216−226.

(8) Qiu, H.; Xu, T.; Wang, Z. L.; Ren, W.; Nan, H. Y.; Ni, Z. H.; Chen, Q.; Yuan, S. J.; Miao, F.; Song, F. Q.; et al. Hopping transport through defect-induced localized states in molybdenum disulphide. *Nat. Commun.* **2013**, *4*, 2642.

(9) Nan, H. Y.; Wang, Z. L.; Wang, W. H.; Liang, Z.; Lu, Y.; Chen, Q.; He, D. W.; Tan, P. H.; Miao, F.; Wang, X. R.; et al. Strong photoluminescence enhancement of MoS_2 through defect engineering and oxygen bonding. *ACS Nano* **2014**, *8*, 5738−5745.

(10) Lu, J.; Carvalho, A.; Chan, X. K.; Liu, H.; Liu, B.; Tok, E. S.; Loh, K. P.; Neto, A. H. C.; Sow, C. H. Atomic healing of defects in transition metal dichalcogenides. *Nano Lett.* **2015**, *15*, 3524−3532.

(11) Wu, Z. T.; Ni, Z. H. Spectroscopic investigation of defects in two dimensional materials. *Nanophotonics* **2017**, DOI: 10.1515/nanoph-2016-0151.

(12) Tongay, S.; Suh, J.; Ataca, C.; Fan, W.; Luce, A.; Kang, J. S.; Liu, J.; Ko, C.; Raghunathanan, R.; Zhou, J.; Ogletree, F.; Li, J. B.;

DOI: 10.1021/acs.jpcc.7b03585
J. Phys. Chem. C 2017, 121, 12294−12299

Grossman, J. C.; Wu, J. Q. Defects activated photoluminescence in two-dimensional semiconductors: Interplay between bound, charged, and free excitons. *Sci. Rep.* **2013**, *3*, 2657.
(13) Atallah, T. L.; Wang, J.; Bosch, M.; Seo, D.; Burke, R. A.; Moneer, O.; Zhu, J.; Theibault, M.; Brus, L. E.; Hone, J.; et al. Electrostatic screening of charged defects in monolayer MoS_2. *J. Phys. Chem. Lett.* **2017**, *8*, 2148−2152.
(14) Cao, Z.; Harb, M.; Lardhi, S.; Cavallo, L. Impact of interfacial defects on the properties of monolayer transition metal dichalcogenide lateral heterojunctions. *J. Phys. Chem. Lett.* **2017**, *8*, 1664−1669.
(15) Feng, L. P.; Su, J.; Li, D. P.; Liu, Z. T. Tuning the electronic properties of Ti−MoS_2 contacts through introducing vacancies in monolayer MoS_2. *Phys. Chem. Chem. Phys.* **2015**, *17*, 6700−6704.
(16) Khondaker, S. I.; Islam, M. R. Bandgap engineering of MoS_2 flakes via oxygen plasma: A layer dependent study. *J. Phys. Chem. C* **2016**, *120*, 13801−13806.
(17) Parkin, W. M.; Balan, A.; Liang, L.; Das, P. M.; Lamparski, M.; Naylor, C. H.; Rodríguez-Manzo, J. A.; Johnson, A. T. C.; Meunier, V. Raman shifts in electron-irradiated monolayer MoS_2. *ACS Nano* **2016**, *10*, 4134−4142.
(18) Srivastava, A.; Sidler, M.; Allain, A. V.; Lembke, D. S.; Kis, A.; Imamoğlu, A. Optically active quantum dots in monolayer WSe_2. *Nat. Nanotechnol.* **2015**, *10*, 491−496.
(19) Zafar, A.; Nan, H. Y.; Zafar, Z.; Wu, Z. T.; Jiang, J.; You, Y. M.; Ni, Z. H. Probing the intrinsic optical quality of CVD grown MoS_2. *Nano Res.* **2017**, *10*, 1608−1617.
(20) Wu, Z. T.; Luo, Z. Z.; Shen, Y. T.; Zhao, W. W.; Wang, W. H.; Nan, H. Y.; Guo, X. T.; Sun, L. T.; Wang, X. R.; You, Y. M.; et al. Defects as a factor limiting carrier mobility in WSe_2: a spectroscopic investigation. *Nano Res.* **2016**, *9*, 3622−3631.
(21) Liu, Y. L.; Nan, H. Y.; Wu, X.; Pan, W.; Wang, W. H.; Bai, J.; Zhao, W. W.; Sun, L. T.; Wang, X. R.; Ni, Z. H. Layer-by-layer thinning of MoS_2 by plasma. *ACS Nano* **2013**, *7*, 4202−4209.
(22) Li, H.; Lu, G.; Wang, Y. L.; Yin, Z. Y.; Cong, C. X.; He, Q. Y.; Wang, L.; Ding, F.; Yu, T.; Zhang, H. Mechanical exfoliation and characterization of single- and few-layer nanosheets of WSe_2, TaS_2, and $TaSe_2$. *Small* **2013**, *9*, 1974−1981.
(23) Jones, A. M.; Yu, H. Y.; Ghimire, N. J.; Wu, S. F.; Aivazian, G.; Ross, J. S.; Zhao, B.; Yan, J. Q.; Mandrus, D. G.; Xiao, D.; et al. Optical generation of excitonic valley coherence in monolayer WSe_2. *Nat. Nanotechnol.* **2013**, *8*, 634−638.
(24) You, Y. M.; Zhang, X.; Berkelbach, T. C.; Hybertsen, M. S.; Reichman, D. R.; Heinz, T. F. Observation of biexcitons in monolayer WSe_2. *Nat. Phys.* **2015**, *11*, 477−481.
(25) Schmidt, T.; Lischka, K.; Zulehner, W. Excitation-power dependence of the near-band-edge photoluminescence of semiconductors. *Phys. Rev. B: Condens. Matter Mater. Phys.* **1992**, *45*, 8989.
(26) Zhang, X. X.; You, Y. M.; Zhao, S. Y.; Heinz, T. F. Experimental evidence for dark excitons in monolayer WSe_2. *Phys. Rev. Lett.* **2015**, *115*, 257403.
(27) Tosun, M.; Chan, L.; Amani, M.; Roy, T.; Ahn, G. H.; Taheri, P.; Carraro, C.; Ager, J. W.; Maboudian, R.; Javey, A. Air stable n-doping of WSe2 by anion vacancy formation with mild plasma treatment. *ACS Nano* **2016**, *10*, 6853−6860.
(28) Yuan, S.; Roldán, R.; Katsnelson, M. I.; Guinea, F. Effect of point defects on the optical and transport properties of MoS_2 and WS_2. *Phys. Rev. B: Condens. Matter Mater. Phys.* **2014**, *90*, 041402.
(29) Komsa, H. P.; Kotakoski, J.; Kurasch, S.; Lehtinen, O.; Kaiser, U.; Krasheninnikov, A. V. Two-dimensional transition metal dichalcogenides under electron irradiation: Defect production and doping. *Phys. Rev. Lett.* **2012**, *109*, 035503.
(30) Komsa, H. P.; Kurasch, S.; Lehtinen, O.; Kaiser, U.; Krasheninnikov, A. V. From point to extended defects in two-dimensional MoS_2: Evolution of atomic structure under electron irradiation. *Phys. Rev. B: Condens. Matter Mater. Phys.* **2013**, *88*, 035301.
(31) Lin, Y. C.; Björkman, T.; Komsa, H. P.; Teng, P. Y.; Yeh, C. H.; Huang, F. S.; Lin, K. H.; Jadczak, J.; Huang, Y. S.; Chiu, P. W.; et al. Three-fold rotational defects in two-dimensional transition metal dichalcogenides. *Nat. Commun.* **2015**, *6*, 6736.
(32) Hong, J. H.; Hu, Z. X.; Probert, M.; Li, K.; Lv, D. H.; Yang, X. N.; Gu, L.; Mao, N. N.; Feng, Q. L.; Xie, L. M.; et al. Exploring atomic defects in molybdenum disulphide monolayers. *Nat. Commun.* **2015**, *6*, 6293.

DOI: 10.1021/acs.jpcc.7b03585
J. Phys. Chem. C 2017, 121, 12294−12299